Kristian Angele 2003 **Experimental studies of turbulent boundary layer separation and control**

KTH Mechanics

S-100 44 Stockholm, Sweden

Abstract

The object of the present work is to experimentally study the case of a turbulent boundary layer subjected to an Adverse Pressure Gradient (APG) with separation and reattachment. This constitutes a good test case for advanced turbulence modeling. The work consists of design of a wind-tunnel setup, development of Particle Image Velocimetry (PIV) measurements and evaluation techniques for boundary layer flows, investigations of scaling of boundary layers with APG and separation and studies of the turbulence structure of the separating boundary layer with control by means of streamwise vortices. The accuracy of PIV is investigated in the near-wall region of a zero pressure-gradient turbulent boundary layer at high Reynolds number. It is shown that, by careful design of the experiment and correctly applied validation criteria, PIV is a serious alternative to conventional techniques for well-resolved accurate turbulence measurements. The results from peak-locking simulations constitute useful guide-lines for the effect on the turbulence statistics. Its symptoms are identified and criteria for when this needs to be considered are presented. Different velocity scalings are tested against the new data base on a separating APG boundary layer. It is shown that a velocity scale related to the local pressure gradient gives similarity not only for the mean velocity but also to some extent for the Reynolds shear-stress. Another velocity scale, which is claimed to be related to the maximum Reynolds shear-stress, gives the same degree of similarity which connects the two scalings. However, profile similarity achieved within an experiment is not universal and this flow is obviously governed by parameters which are still not accounted for. Turbulent boundary layer separation control by means of streamwise vortices is investigated. The instantaneous interaction between the vortices and the boundary layer and the change in the boundary layer and turbulence structure is presented. The vortices are growing with the boundary layer and the maximum vorticity is decreased as the circulation is conserved. The vortices are non-stationary and subjected to vortex stretching. The movements contribute to large levels of the Reynolds stresses. Initially non-equidistant vortices become and remain equidistant and are confined to the boundary layer. The amount of initial streamwise circulation was found to be a crucial parameter for successful separation control whereas the vortex generator position and size is of secondary importance. At symmetry planes the turbulence is relaxed to a near isotropic state and the turbulence kinetic energy is decreased compared to the case without vortices.

Descriptors: Turbulence, Boundary layer, Separation, Adverse Pressure Gradient (APG), PIV, control, streamwise vortices, velocity scaling.

Preface

This thesis considers experiments in turbulent boundary layers with and without pressure gradient. Pressure gradient induced separation and its control by means of streamwise vortices is considered.

Paper 1. K. P. Angele and B. Muhammad-Klingmann 2003. Accurate PIV measurements in the near-wall region of a turbulent boundary layer at high Reynolds number. Submitted to *Experiments of Fluids*.

Paper 2. K. P. Angele and B. Muhammad-Klingmann 2003. The effect of peak-locking on the accuracy of turbulence statistics in digital PIV. Submitted to *Experiments of Fluids*.

Paper 3. K. P. Angele and B. Muhammad-Klingmann 2003. Self-similarity velocity scalings in a separating turbulent boundary layer. Selected paper at European Turbulence Conference IX. To be submitted for journal publication.

Paper 4. K. P. Angele and F. Grewe 2002. Streamwise vortices in turbulent boundary layer separation control. Selected paper at 11th International Symposium on Application of Laser Techniques to Fluid Mechanics, Lisbon. Submitted to *Experiments of Fluids*.

Paper 5. K. P. Angele 2003. The effect of streamwise vortices on the turbulence structure of a separating boundary layer. To be submitted for journal publication.

Division of work by authors

Paper 1. The measurements were carried out by Kristian Angele in the setup designed and built by Dr. Jens Österlund. The evaluation of the data was done by Kristian Angele and the writing of the paper was done by Kristian Angele and Barbro Muhammad-Klingmann. Dr. Jens Österlund is highly acknowledged for the use of the hot-wire data for comparison. This work has partly been presented by K. Angele and published in: K. Angele & B. Muhammad-Klingmann 1999. The use of PIV in Turbulent Boundary Layer Flows. In *Geometry and Statistics of Turbulence, Proc. of IUTAM Symposium.* November 1-5 1999 Hayama. Eds: T. Kambe, T. Nakano and T. Miyaushi. Kluwer Academic Publishers. K. Angele & B. Muhammad-Klingmann 2000. PIV measurements in a high Re turbulent boundary layer. In *Advances in Turbulence VIII, Proc. of the ETC8*, Barcelona June 27-30 2000. Ed: C. Dopazo. This work has also partly been presented by K. Angele at the conference: Svenska Mekanik dagarna, Stockholm, Sweden June 7-9 1999. PIVNet T5/ERCOFTAC SIG 32, Rome Italy, September 3-4 1999.

Paper 2. The simulations were carried out by Kristian Angele and the writing of the paper was done by Kristian Angele and Barbro Muhammad-Klingmann.

Paper 3. The work on turbulent boundary layer separation was initiated by Docent Barbro Muhammad-Klingmann on the basis of preliminary studies by Jonas Gustavsson. The experimental setup was designed by Kristian Angele and built and manufactured with aid from Kyle Mowbray, Markus Gällstedt and Ulf Landén. The experiments were carried out by Kristian Angele. The evaluation of the data was done by Kristian Angele. The results were discussed with Barbro Muhammad-Klingmann. The writing of the paper was mainly done by Kristian Angele. This work has partly been presented by Kristian Angele and published in: K. Angele & B. Muhammad-Klingmann 2001. PIV measurements in a separating turbulent APG boundary layer. In *Turbulence and Shear Flow Phenomena 2, Proc. of TSFP-2 Vol.III*, Stockholm June 27-29 2001. Eds: E. Lindborg, A. V. Johansson, J. Eaton, J. Humphry, N. Kasagi, M. Leschziner, M. Sommerfeld. K. Angele 2002. Pressure-based scaling in a separating turbulent APG boundary layer. In *Proc. European Turbulence Conference-ETC 9*, Southampton July 2-5 2002. Eds: I. P. Castro, P. E. Hancock and T. G. Thomas.

Paper 4. This cooperation was initiated by Professor Arne Johansson, KTH Mechanics and Professor H.-H. Fernholz at the Hermann-Föttinger-Institut für Strömungsmechanik Technische Universität, Berlin, Germany. The setup was designed at the HFI by Frank Grewe and Professor H.-H. Fernholz. The measurement equipment such as the pulsed-wires and the wall shear-stress fence

were designed and built in-house at the HFI. This work has been carried out during three visits, in total six months, at the HFI during 2001-2002. All the people at HFI are highly acknowledged. This work was done in cooperation with Frank Grewe. The experiments were carried out by Kristian Angele and Frank Grewe. The evaluation of the data and the writing of the paper was mainly done by Kristian Angele. The data for the uncontrolled case were captured earlier by Frank Grewe. This work has partly been presented by Frank Grewe and published in: K. Angele & F. Grewe 2002. Investigation of the streamwise vortices from a VG in APG separation control using PIV. In *Proc. 11th International Symposium on Application of Laser Techniques to Fluid Mechanics*, Lisbon July 8-11 2002.

Paper 5. The experiments and the evaluation of the data were carried out by Kristian Angele. The results were discussed with Barbro Muhammad-Klingmann. The writing of the paper was mainly done by Kristian Angele. This work has partly been presented by Kristian Angele at the conference: American Physical Society Division of Fluid Dynamics 55th Annual Meeting, Dallas November 24-26 2002. It will be presented by Kristian Angele at TSFP3, Sendai June 25-27 2003.

x

Contents

CHAPTER 1

Introduction

Turbulent boundary layer separation is a complex flow phenomenon which greatly affects the performance in many technical applications. For instance, the maximum efficiency, in terms of lift on an air-foil at a high angle of attack, is often at an operational point close to the onset of separation. Some other practical examples where separation can occur are in engine inlet diffusers, on the blades in turbo machinery, in exhaust nozzles and on wind turbine blades. In all these cases, separation reduces the pressure recovery and increases the drag. Therefore, there is much to be gained if separation can be fully understood, predicted and possibly controlled. Separation can be induced by flow around a sharp corner. In boundary layers with an Adverse Pressure Gradient (APG), separation occurs when the flow near the surface can no longer withstand the downstream pressure rise. The parameters involved in predicting separation in this case involve the geometry, non-local history effects, large streamline curvature and low frequency unsteadiness such as vortex shedding. All these features are typically difficult to capture with turbulence models and experimental work is therefore important, both to increase the understanding of the flow itself and for validation of turbulence models. An increased knowledge about separation is also important for separation control purposes. Separation control is today striving towards more complex active and reactive methods to minimize the additional drag associated with conventional mixing devices such as vortex generators. However, a deeper understanding of the interaction between streamwise vortices and a separating turbulent boundary layer, especially in terms of instantaneous vortex behaviour and the turbulence structure of the boundary layer, is still lacking. In the following chapters the fields of turbulent boundary layers, APG and separation are introduced. Thereafter, scaling of tubulent boundary layers and separation control are reviewed separately followed by brief introductions to the existing methods of separation prediction by means of simulations and measurements. The final chapter is devoted to a description of the design of the present experimental setup and a summary of the contributions to the field.

Turbulent boundary layer

Nearly hundred years ago Prandtl published a paper on the concept of *boundary layers* which revolutionized the field of fluid dynamics. The formation of a boundary layer is due to the no-slip condition *i.e.* no discontinuity in velocity can exist between the moving fluid and a boundary due to the friction caused by the viscous nature of fluids. When the flow is decomposed into a mean and a fluctuating part (Reynolds decomposition), the equations governing the mean flow in an incompressible, two-dimensional, steady boundary layer are the continuity equation

$$\frac{\partial U}{\partial x} + \frac{\partial V}{\partial y} = 0 \tag{2.1}$$

and the turbulent boundary layer equation

$$U\frac{\partial U}{\partial x} + V\frac{\partial U}{\partial y} = -\frac{1}{\rho}\frac{dP}{dx} + \frac{\partial}{\partial y}\left(\nu\frac{\partial U}{\partial y} - \overline{u'v'}\right). \tag{2.2}$$

Capital letters correspond to mean quantities and lower case letters with a prime denotes fluctuations. The overbar in $\overline{u'v'}$ denotes a time average. The space is described by x, y and z and the solution we seek is for the velocity components in these directions U, V, W. The physical properties of the fluid are the density ρ and the viscosity ν. The boundary condition at the wall is expressed as

$$U(x, y = 0) = 0 \qquad\qquad V(x, y = 0) = 0. \tag{2.3}$$

At the second boundary, the outer edge of the boundary layer, the undisturbed velocity, or the free-stream velocity, is reached asymptotically

$$U(x, y/\delta \to 1) \to U_\infty \tag{2.4}$$

where δ is the boundary layer thickness, see figure 2.1. The boundary layer thickness is much smaller in magnitude than the typical downstream scale. This implies that the static pressure can be assumed to be constant through-out the boundary layer in the wall-normal direction.

Although turbulence is often treated in statistical terms, it is not an entirely random phenomenon. Flow visualizations, such as the one shown in figure 2.2, gives qualitative evidence of the existence of coherent structures. With the fast development of Direct Numerical Simulations (DNS) and PIV,
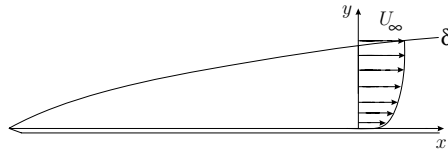
FIGURE 2.1. The turbulent boundary layer on a flat plate. Flow is from left to right. The vertical size of the boundary layer is exaggerated.
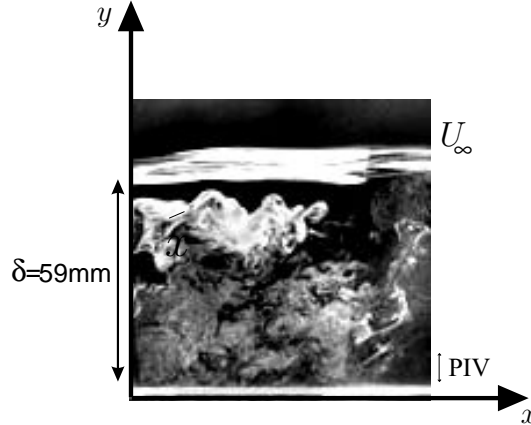
FIGURE 2.2. Smoke visualization of a zero pressure-gradient turbulent boundary layer. The flow is from left to right and the plate is at the bottom of the picture. The upper streak of smoke corresponds to the free-stream.

quantitative information about such structures can be achieved. In the ZPG turbulent boundary layer, where the first term on the right hand side of equation (1) is zero, coherent structures such as hair-pin vortices are known to exist in the near-wall region. Adrian *et al.* (2000) recently conducted well resolved PIV measurements covering the whole boundary layer in a ZPG case and concluded that packets of hair-pin vortices occur in the outer region. This has also been observed in DNS of channel flow by Zhou *et al.* (1999). Another well-established fact is that low-speed streaks exist in the near-wall region with a characteristic spanwise spacing of $\lambda^+=100$ (in viscous scaling). Recently Österlund *et al.* (2002) found that the relative importance of these streaks decrease as the Reynolds number increases. Wall shear-stress measurements conducted with a hot-film array showed no evidence of streaks for sufficiently high Reynolds number, however, when subjected to appropriate filtering they

3

revealed streaks of approximately $\lambda^+=100$. The ability of PIV for capturing coherent structures is exemplified in chapter 7.3.

The APG boundary layer and separation

In a boundary layer where the pressure gradient, *i.e.* the first term on the right hand side of equation (1), is non-zero and positive, the flow is said to be subjected to an Adverse Pressure Gradient (APG). The pressure coefficient is defiened as

$$c_p = \frac{P - P_{ref}}{P_0 - P_{ref}} \qquad (3.5)$$

where P is the mean wall static pressure, P_0 the total, or stagnation pressure, and P_{ref} is a reference wall static pressure. The fact that the static pressure is constant through-out the boundary layer in the wall-normal direction gives rise to a larger deceleration close to the wall where the flow carries less momentum. The skin-friction coefficient

$$c_f = \frac{\tau_w}{\frac{1}{2}\rho U_\infty^2} = 0 \qquad (3.6)$$

based on the wall shear-stress, τ_w, decreases as a consequence of this, see figure 3.1 (a). This also implies that the shape of the profile is changed, best displayed in terms of the increase in the shape-factor, $H_{12} = \delta^*/\theta$, based on the displacement thickness

$$\delta^* = \int_0^\infty \left(1 - \frac{U(y)}{U_\infty}\right) dy, \qquad (3.7)$$

and the momentum-loss thickness

$$\theta = \int_0^\infty \frac{U(y)}{U_\infty} \left(1 - \frac{U(y)}{U_\infty}\right) dy, \qquad (3.8)$$

see figure 3.1 (b). The largest gradient in the mean velocity profile moves out from the wall as the flow develops towards separation. This completely changes the character of the flow. The near-wall turbulence generation is weakened and the spanwise spacing of the of sub-layer streaks increases, see Simpson *et al.* (1977) and Skote (2002). Skote (2002) reported an increase from $\lambda^+ = 100$ at $H_{12} = 1.4$ to $\lambda^+ = 130$ at $H_{12} = 1.6$ and Simpson *et al.* (1977) reported a value of 100 based on the velocity scale U_m of Perry & Schofield (1973), which is proportional to the maximum Reynolds shear-stress which is drastically increased in APG, see chapter 4.2. Ultimately the streaks disappear at separation, see Skote (2002). The wall-normal distributions of the Reynolds stresses are quite

5
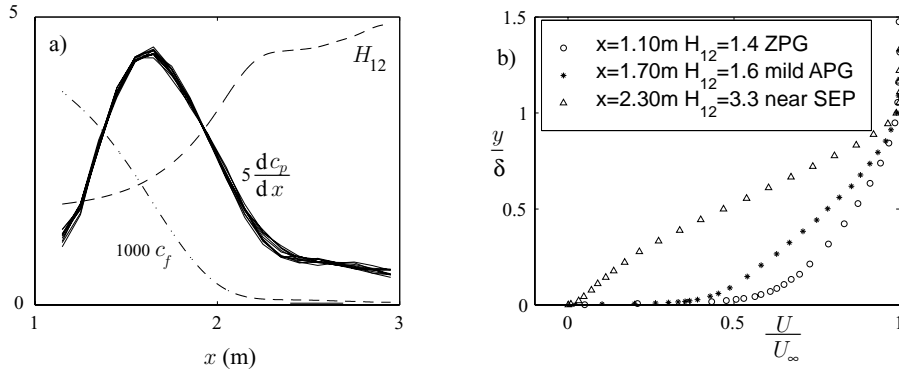
FIGURE 3.1. (a) Pressure gradient, dc_p/dx, skin-friction coefficient, c_f, and the shapefactor, H_{12} obtained by solving the von Karman momentum integral equation with the pressure distribution as input. (b) LDV mean velocity profiles of the streamwise velocity component. These results are presented in paper 4.
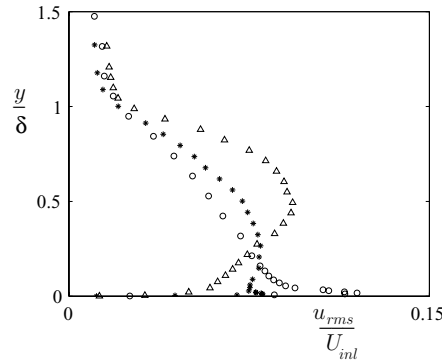
FIGURE 3.2. u_{rms} profile measured with LDV scaled with U_{inl}, the free-stream velocity at x=1.10 m. Symbols as in figure 3.1 (b).

different from the ZPG case, with large peaks in the middle of the boundary layer. Figure 3.2 shows the root-mean-square velocity, u_{rms}. The typical feature of APG boundary layers is shown: the gradual disappearing of the near-wall peak and the emergence of a new peak induced by the inflection point of the streamwise mean velocity profile. As H_{12} increases, the position of this peak moves away from the wall in terms of y/δ.

6
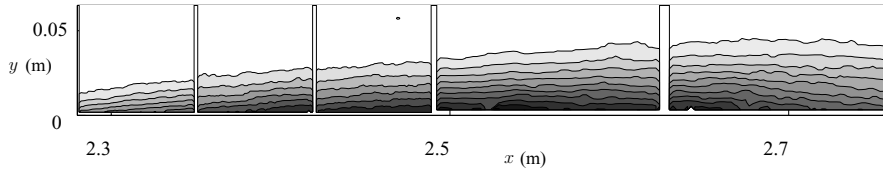
FIGURE 3.3. Contour plot of the backflow coefficient, χ, in the shallow separation bubble presented in paper 4. Flow is from left to right. Each contour corresponds to 5% increase in χ. The flow is separated between x=2.4 m and x=2.7 m.

Schubauer & Spangenberg (1960) investigating the effect of different pressure distributions on the boundary layer development, separation and pressure recovery. They observed that an initially steep and progressively relaxed APG gives the highest pressure recovery in the shortest distance. This implies that the boundary layer can withstand a stronger pressure gradient at an early stage when it is not yet affected but becomes less resistant as the profile has been changed.

If the pressure gradient is strong and persistent the flow ultimately shows similarities to a mixing layer and separates. APG induced separation is a continuous process, with intermittent instantaneous backflow upstream of the mean separation point, as opposed to the case where the flow separates at a sharp corner (see the last section). According to the extensive review by Simpson (1989), steady two-dimensional separation is defined by c_f=0 and χ_w=50%. χ_w is the backflow coefficient in the vicinity of the wall. It is defined as the amount of time (with respect to the total time) the flow spends in the upstream direction.

Following Alving & Fernholz (1996), we may define three different types of separation:

- Mild APG induced separation
- Strong APG induced separation
- Geometry induced separation (here referred to as sharp corner induced separation).

3.1. Mild APG induced separation

If the separated shear layer is reattached to the surface, a closed region of mean backflow is formed, often called a separation bubble. In the present study the flow is close to the zero wall shear-stress case, investigated by Stratford (1959a), Stratford (1959b) and Dengel & Fernholz (1990), with a shallow separation bubble, illustrated in figure 3.3. Different definitions exist on a separation bubble. Some are the region bounded by: the zero streamline (based

7
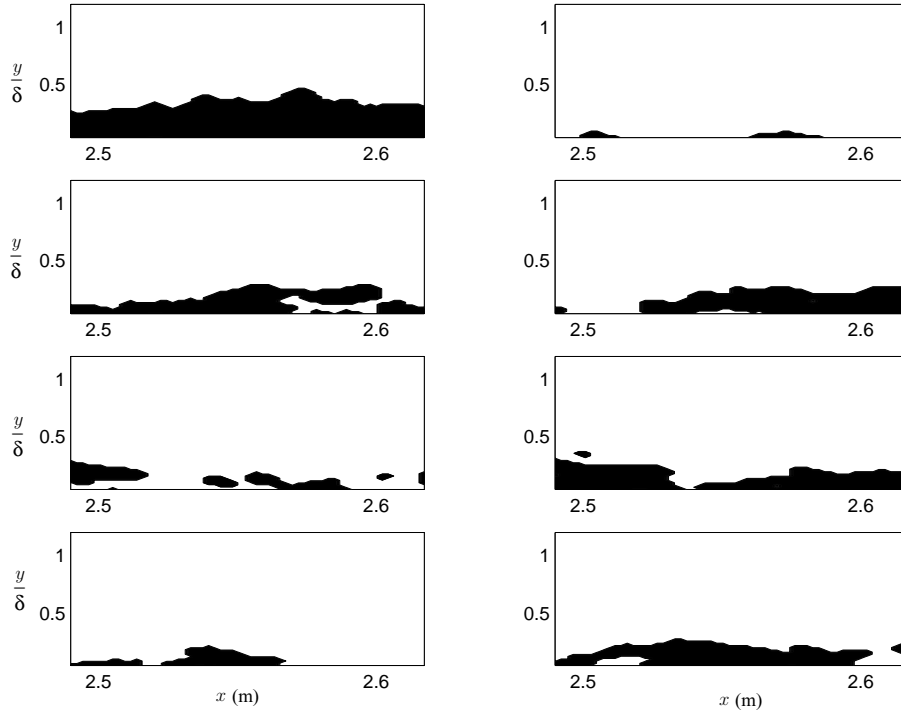
FIGURE 3.4. Eight flow fields evaluated from PIV showing the instantaneous direction of the flow. Black refers to flow in the negative x-direction, *i.e.* backflow and white corresponds to flow in the positive x-direction.

on the stream function), the contour of the backflow coefficient equal to 50% or the mean velocity equal to zero. For a discussion on this, see Törnblom (2003). Figure 3.4 shows a sequence of eight flow fields in terms of the instantaneous backflow. This shows how the mean separated region is built up of fundamentally different scenarios ranging from attached flow to separated flow. This is similar to what has been observed in the plane asymmetric diffuser, (see below). At some instances the flow is separated in small regions (not necessarily at the wall) with attached flow between, showing the three-dimensional nature of instantaneous separation. The DNS by Na & Moin (1998) showed that the instantaneous separation is a highly three-dimensional process without a clear separation and reattachment line and the two-dimensional mean bubble is merely a consequence of time averaging.

Dengel & Fernholz (1990) investigated three different cases with flow very close to zero wall shear-stress. An axi-symmetric setup was used to minimize

three-dimensional effects which can be troublesome in separated flows. Focus was on the proper mean velocity scaling and this paper is reviewed in more detail in chapter 4.2. They conclude from correlation measurements that the integral length scales indicate large scales structures which govern the separated shear layer. Alving & Fernholz (1995) and Alving & Fernholz (1996) continued this work but the setup was modified to get an earlier separation to be able to study the relaxation of the boundary layer after reattachment. The separation definition by Simpson (1989) was shown to hold also at reattachment. They suggested that vertical oscillations of the separated shear layer at reattachment might take place, a flapping motion which have been observed in many other types of separation. They suggest that the large scales in the outer region survive separation and disturb the relaxation of the inner stresses to a ZPG state. Grewe (private communication) again re-built the test section and conducted the measurements on a mild APG separation bubble which are referred to as the uncontrolled case in paper 4. Hot-wire measurements in the separated shear layer reveal a peak in the frequency spectra at f=25 Hz, which is believed to be associated with the natural shear-layer (Kelvin-Helmholz) instability. The observed frequency corresponds to a $f\delta/U_\infty \approx 0.15$ based on the characteristics of the separating shear layer. This is similar to the value obtained by Na & Moin (1998) ($f\delta^*_{inl.}/U_\infty$=0.001-0.0025) based on the inlet conditions.

The plane asymmetric diffuser, see Buice & Eaton (1996), Kaltenbach *et al.* (1999) and Törnblom (2003), is a flow case which is somewhere between the mild APG and a sharp corner induced separation (see below). The geometry consist of two channels with different height with a gradual area increase, a diffuser with one inclined wall. If the corner is not sharp the flow can handle this as long as the opening angle is not too large. The flow separates on the inclined wall and reattaches downstream of it in the beginning of the downstream channel. The separated shear layer above the bubble has strong gradients where the turbulence production and kinetic energy is intensified. The backflow is intermittently supplied to the bubble and the instantaneous flow is ranging from fully separated to fully attached.

3.2. Strong APG induced separation

A simple example of strong APG induced separation is the flow behind a circular cylinder, which can be thought of as an extreme case of an air-foil at stall. In a certain range of Reynolds numbers, large scale vortices from the separated shear layers on each side of the cylinder, are convected downstream. This process is called vortex shedding and this specific case is called the Von $Karman$ vortex street. The vortex shedding has a certain non-dimensional frequency based on the flow conditions and the geometry, $fd/U_\infty \approx 0.2$, the Strouhal number.

If the flow is subjected to a strong and persistent pressure gradient this often leads to a large separated region associated with a large streamline curvature where the shear layer breaks away from the surface. If this flow does not reattach, a wake is formed, as in the case of a cylinder. Unsteadiness or a low frequent flapping motion of the separated region (slower than the inverse time scale of the largest eddies) is a common feature, see Dianat & Castro (1989, 1991). Characteristic for many of the strong APG separation experiemnts is the significance of the normal stresses for the turbulence production, see Simpson *et al.* (1977), Simpson *et al.* (1981*a*), Na & Moin (1998) and Skote (2002).

Much work on strong APG induced separation has been conducted by the group lead by Simpson, see for example Simpson *et al.* (1977), Simpson *et al.* (1981*b*), Simpson *et al.* (1981*a*) and Shiloh *et al.* (1981). These are pioneering works including directionally sensitive measurements inside a strong separated region. The turbulence intensity and production in the outer separated shear layer was found to be high and the backflow and its turbulence in the inner region was supplied from these large scales by turbulent diffusion. No turbulent production occurs in the near wall region. It was also suggested that the growth of the boundary layer is, like in a mixing layer, caused by turbulent diffusion from the middle region. In this kind of flow, the mean features are merely a consequence of time averaging, which means that the turbulence modeling based on the local velocity gradient is not likely to work. The higher order moments skewness (S) and flatness (F), were also presented for the first time. The ZPG features of these: a minimum in F_u coinciding with the maximum in u_{rms} and S_u=0, disappear as the significance of the near wall region is reduced and S_u becomes negative in the separated region. S_v is essentially the mirror image of S_u whereas F_u and F_v were not so much affected by separation. Transverse velocity and turbulence showed that S_w was zero within the measurement accuracy, which should be the case in a two-dimensional flow. F_w was found to be similar to F_u and F_v.

3.3. Separation induced by a sharp corner

Separation occurs when there is a sudden change in geometry, *e.g.* behind blunt bodies such as buildings or vehicles where a wake is formed. Internal flows with an area change, as for example a pipe with a sudden change in diameter or a diffuser with a gradually increasing cross-section area, are other examples. Some generic cases in fluid dynamic research, where numerous experiments have been conducted are presented in figure 3.5. The first example is the backward facing step, figure 3.5 (a), where two channels with different cross-section area are connected. The sudden area change causes the flow to separate at the corner and form a recirculation zone at high Reynolds number. Reattachment follows downstream of the step. The reattachment length being approximately six step heights. This is a common test-case for turbulence modeling. Some other
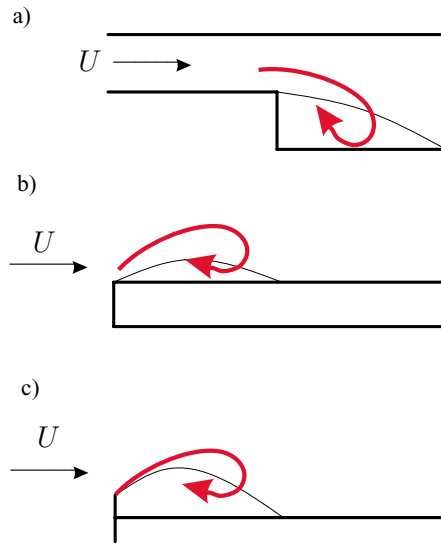
FIGURE 3.5. Separation induced by a sharp corner (a) backward facing step (b) blunt flat plate (or cylinder) and (c) fence with splitter plate.

simple geometries that have been used are the blunt flat plate (or cylinder), figure 3.5 (b), at zero angle of attack, where the flow separates at the leading edge corners and reattaches if the plate is long enough, see Kiya & Sasaki (1983). The bluff plate (or fence) normal to the flow followed by a splitter plate parallel to the flow, is shown in figure 3.5 (c). The flow separates at the corner and reattachment occurs at the splitter plate, see Hancock (2000) for recent experiments and an extensive review on earlier experiments, as for example that of Ruderich & Fernholz (1986). Another recent experiment is presented by Hudy & Naguib (2003). A fence placed on a flat plate, along which a boundary layer develops, is another example, see for example Sonnenberger (2002). What characterizes all these cases is that the separation line is fixed and does not fluctuate as is the case of the reattachment line, which makes the process of separation less complicated than in a case where both the reattachment and separation line fluctuate in time. Large scales associated with a low frequency and a flapping motion of the reattaching shear layer are common features observed in most experiments.

Turbulent boundary layers and scaling

In laminar boundary layers belonging to the family of Falkner-Skan flows, including the ZPG Blasius case, the governing equations can be reduced to an ordinary differential equation when scaled with the proper velocity and length scales. This means that the velocity profiles at different downstream positions are self-similar when scaled with these scales. A turbulent boundary layer on the other hand is more complex and can not be reduced in this manner. Yet, similarity arguments and dimensional analysis can give some insight. Historically, one way to increase the understanding of turbulent boundary layer flow has therefore been to investigate the scales governing the flow. The concept of self-similarity has also proven to be fruitful.

4.1. The inner region

A turbulent boundary layer is empirically found to be governed by different scales in different regions of the layer. The *inner* region close to the wall is dominated by viscous forces and the inertia terms on the left hand side of equation (1) can be neglected. This region is usually scaled with the friction velocity, $u_\tau = \sqrt{\tau_w/\rho}$ based on the wall shear-stress and the density. In the ZPG case, the mean velocity profiles in the inner part of the boundary layer are self-similar and described by $U^+ = f(y^+)$ where $U^+ = U/u_\tau$ and $y^+ = yu_\tau/\nu$. Close to the wall, $y^+ \leq 5$, the velocity profile is linear, $U^+ = y^+$, and in a region of constant total shear-stress $\tau^+ \equiv \frac{\partial U^+}{\partial y^+} + \overline{u'v'^+} = 1$, $U^+ = \kappa^{-1} \ln y^+$. This is referred to as the logarithmic law of the wall. However, in APG the pressure gradient is not zero and the equation for the inner region scaled with u_τ has the form

$$\tau^+ = 1 + \lambda y^+, \qquad \lambda = \left(\frac{u_{ps}}{u_\tau}\right)^3, \qquad u_{ps} = \left(\frac{\nu}{\rho}\frac{dP}{dx}\right)^{1/3}. \qquad (4.9)$$

The influence of the pressure gradient on the total shear stress is reflected in λ, the ratio between a viscous pressure gradient velocity scale u_{ps} and u_τ. This gives rise to a mixed logarithmic and square-root behaviour in the overlap region which, expressed in viscous scaling, has the form

$$U^+ = \frac{1}{\kappa}\left[\ln y^+ - 2\ln\frac{\sqrt{1 + \lambda y^+} + 1}{2} + 2\left(\sqrt{1 + \lambda y^+} - 1\right)\right] + B_{APG}. \qquad (4.10)$$
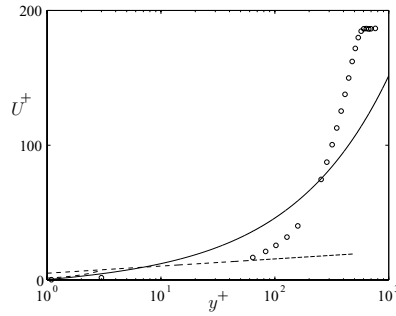
FIGURE 4.1. Pressure gradient scaling for the inner and over-lap region upstream of separation (H_{12}=3.33). The solid line corresponds to equation (4.10) and the dashed lines to the linear and logarithmic regions. One can see that the departure from the logarithmic law is at least in qualitative agreement with the present data.

The suaqre-root function was first suggested by Stratford (1959b) based on mixing-length theory. This was verified by Stratford (1959a) in an experiment where the boundary layer was on the verge of separation. Equation (4.9) has been derived by different means in numerous studies for example Townsend (1961), McDonald (1969), Kader & Yaglom (1978) and Skote (2002). As $\lambda\rightarrow0$, the logarithmic law for the flow without pressure gradient is asymptotically reached. Simpson $et\ al.$ (1977) showed that the logarithmic region vanishes at the same position as the first backflow events appear in the vicinity of the wall. This was verified later by Dengel & Fernholz (1990). As $\lambda\rightarrow\infty$, (as separation is approached), u_τ is vanishing and a singularity appears when using u_τ for scaling.

Simpson $et\ al.$ (1981b) showed that the backflow inside a separated region can be scaled with the maximum negative velocity and its distance from the wall. Skote (2002) claimed that equation (4.10) changes to

$$U^+ = \frac{1}{\kappa}\left[2\sqrt{\lambda y^+ - 1} - \arctan\sqrt{\lambda y^+ - 1}\right] + D_{APG} \qquad (4.11)$$

by allowing negative values of u_τ.

4.2. The outer region

4.2.1. *Equilibrium boundary layers*

The outer region has been less extensively investigated. It is usually scaled in velocity-defect form:

$$\frac{U_\infty - U}{u_\tau} = F\left(\eta\right) \qquad\qquad \frac{-\overline{u'v'}}{u_\tau^2} = R\left(\eta\right) \qquad (4.12)$$

$$\eta = \frac{y}{\Delta} \qquad\qquad \Delta = \frac{\delta^* U_\infty}{u_\tau}. \qquad\qquad (4.13)$$

For a boundary layer with pressure gradient, assuming solutions on this form, plugging into equation (1), neglecting the viscous term, leads to

$$-2\beta F - (1+\beta)\eta\frac{\partial F}{\partial \eta} = \frac{\partial R}{\partial \eta} \qquad\qquad \beta = \frac{\delta^*}{\tau_w}\frac{\partial P}{\partial x} \qquad\qquad (4.14)$$

in the limit of Re→∞, see Townsend (1961). The mathematical criterion for similarity solutions to exist is that the parameter β is constant. β represents a ratio of the pressure gradient and the wall shear-stress. With increasing β, the influence of the pressure gradient is increasing. β has a similar role as λ in equation (4.10) and the ratio between these two parameters are the ratio between an outer (δ^*) and the inner (ν/u_τ) length scale. A turbulent boundary layer which is self-similar in this manner is said to be in *equilibrium*. Clauser (1954) investigated one ZPG case and two mild APG turbulent boundary layers and concluded that this kind of similarity exists. Mellor & Gibson (1966) and Mellor (1966) obtained solutions for the velocity defect profile with β as a parameter.

$$u_p = \sqrt{\frac{\delta^*}{\rho}\frac{dP}{dx}} = u_\tau\beta^{1/2} \qquad\qquad (4.15)$$

was used to avoid the singularity when u_τ=0 and $\beta = \infty$. Other experiments were made by for example Watmuff & Westphal (1989), however, the by far most extensive experiment was done by Skåre & Krogstad (1994) who performed experiments in strong APG, however, still without backflow. The mean velocity profiles and the turbulent stresses up to triple correlations were found to be self-similar. It was also shown that $-\overline{u'v'}^+{}_{max}=1+\frac{3}{4}\beta$ and it was pointed out that alternative scalings like $-\overline{u'v'}/\overline{u'v'}_{max}$ are also possible.

Elsberry *et al.* (2000) tried to reproduce the flow of Stratford (1959b,a), however, there are several things which indicate that the flow is far from separation. The shapefactor was constant and the integral lengths scales were approximately linearly increasing in the downstream direction indicating that the flow is in equilibrium, however, the different fluctuating velocity components were governed by different scales.

4.2.2. *Historical effects*

However, a boundary layer developing towards separation is not in equilibrium and is continuously changing. Coles (1956) tried to overcome this problem by developing a linear combination of the logarithmic law of the wall and an outer wake profile based on empirical evidence. This scaling has been proved to be successful in moderate pressure gradients, where the logarithmic region is still present, but as separation is approached it has been shown to be less successful, see for example Dengel & Fernholz (1990). A problem when it comes to a

developing turbulent boundary layer is that the flow might suffer from historical effects. Perry *et al.* (1966) and Perry (1966) divided the turbulent boundary layer into an inner wall region, where the flow is only determined by local flow parameters, and an outer historical region where the flow also might depend on historical effects. Kader & Yaglom (1978) assumed a moving-equilibrium for non-separated flows, to overcome the problems with historical effects. The free-stream velocity was assumed to vary slowly in the downstream direction so that the boundary layer always have time to adjust to this variation. A similar pressure gradient based velocity scale as the one shown in equation (4.15) was introduced for the outer region, however δ^* was replaced by δ in u_p. Yaglom (1979) used the geometric mean value between the modified u_p and u_τ as the velocity scale.

4.2.3. *Other scalings*

A different approach has been taken by Perry & Schofield (1973), Schofield (1981) and Schofield (1986). They claimed that all velocity scales which are depending on the local pressure gradient are not appropriate and instead introduced a velocity scale u_s which explicitly depends on the maximum shear-stress. This velocity scale should replace u_τ when $-\overline{u'v'}^+_{max} \geq 1.5$. u_s was claimed to be the natural velocity scale of the square-root part of the velocity profile in strong APG in a similar way as u_τ is the natural velocity scale of the logarithmic part of the velocity profile in ZPG or mild APG according to Clauser (1954). u_s was determined from a fit to the velocity profile in a similar manner to u_τ from a Clauser plot. A vast amount of experimental data was claimed to confirm the scaling and it is valid after separation as well if the dividing stream-line is taken as y_0 (the position of the wall). Dengel & Fernholz (1990) proposed an asymptotic separation profile based on the same scale which was different from the original universal profile. A 7th order polynomial was found to give a better fit to their data than the original profile suggested by Perry & Schofield (1973), indicating that there is no universal scaling. Only the profiles in the vicinity of separation showed similarity. u_s was still determined by a fit to the profile but the relation to the maximum turbulent shear was not verified. Instead a linear relation between u_s and the backflow coefficient, χ_w was found. A linear relation was also found between χ_w and H_{12}. This scaling was later verified by Alving & Fernholz (1995) at reattachment. However, u_s was not taken from a fit to the square-root part of the profile, even though they claim it is present, but rather chosen to get the best fit to the profile suggested by Dengel & Fernholz (1990). The correlation between the pressure gradient based velocity scale u_p and u_s was poor and this scaling was therefore never shown.

Castillo & Geroge (2001) analyzed the equation for the outer region in a similar manner to Townsend (1961). However, the appropriate length scale was chosen as δ, and the appropriate velocity scale was determined by requiring that

15

the differential equation should be independent of the downstream direction. It was concluded that U_∞ is the appropriate velocity scale (for a flow with fixed upstream conditions) if $\delta \propto U_\infty^{-1/\Lambda}$ where $\Lambda = \delta/(\partial\delta/\partial x)(dc_p/dx)$ is a constant. They reviewed experimental data and claimed that Λ only can have three different values, one for the case of a favorable pressure gradient (FPG), one for APG and one for ZPG. However, the value of Λ is not constant and the profiles are not self-similar when scaled in this manner.

CHAPTER 5

Separation control

Recently, interest has been directed towards control of fluid flow. Usually the aim is to minimize the drag. In laminar flow this often means to delay transition, however, in some cases, forced transition can increase the overall efficiency. This is due to the superior ability of a turbulent boundary layer to stay attached to the surface as compared to the laminar ditto. In turbulent wall-bounded flow, drag reduction means to suppress the turbulence generation mechanism at the wall and when controlling separation the goal is to avoid the loss of lift on for example a wing or to increase the pressure recovery in a diffuser.

One way to classify control is as *reactive*, *active* or *passive* control, see Gad-El-Hak (2000). Generally, an *active* method adds energy to the flow whereas a *passive* extracts energy from the flow for control purposes. A *reactive* method extracts information from the flow by means of sensors and, based on this information, maneuvers actuators for control of the flow. Since the scales in the flow are usually small, active control in experiments utilize miniature sensors, so called Micro Electric Mechanical Systems (MEMS), see for example Yoshino *et al.* (2002). One example is a hot-film array for measuring the instantaneous wall shear-stress in the spanwise direction. A common actuator in experiments is a spanwise slit through which blowing and suction is employed. While reactive control of transition is fairly advanced when using DNS, see Högberg (2001), experiments are still relying on simpler techniques, Lundell (2003). Passive turbulence control, by adding polymers to the flow, has been shown to reduce the drag in turbulent pipe flow, see Hoyt & Sellin (1991) and Smith & Tiederman (1991). Active turbulence control however, is more complicated due to the small spatial turbulence scales, the fast lapses and the generally random behaviour. DNS can be utilized to explore different control algorithms since one has total information about the whole flow field at all times and can employ actuators which would not be realizable in an experiment. Experimental active turbulence control in fully developed turbulent flows is still a challenging task but progress is being made, Fukugata & Kasagi (2002). Since separation is usually accompanied by a decrease in performance, control is desirable. The aim of separation control can, simply stated, be to eliminate the mean reverse-flow *i.e.* to change the flow direction close to the

surface. This can be realized by a variety of techniques. Some examples are to redirect the flow towards the surface, introduce vortical structures which enhance momentum transfer towards the wall or add momentum directly near the wall. For extensive reviews and a vast amount of references on separation control see for example Gad-El-Hak & Bushnell (1991) or the book by Gad-El-Hak (2000).

5.1. Passive techniques

Traditionally, separation control has been based on passive techniques. The reason for this is that the implementation requires less effort and no external energy has to be added to the flow since the passive technique by definition extract energy from the flow itself. Different kinds of fixed devices promoting mixing exist. A fixed device induce a penalty drag at the same time, which has to be smaller than the drag reduction in order to achieve a net gain.

5.1.1. Vortex generators

Schubauer & Spangenberg (1960) investigated the relative performance of many different mixing devices for separation control in a flat plate turbulent boundary layer subjected to a strong APG. The general conclusion was that forced mixing had a similar effect as a lowering of the pressure gradient had. The advantage of using forced mixing is that a larger pressure rise can be achieved in a shorter distance.

The by far most common technique in practical use, on for example wings of commercial air-crafts, is the Vortex Generator (VG) which introduce streamwise vortices. A VG consists of a rectangular or triangular planform, of the order of the local boundary layer thickness, mounted normal to the surface and at an angle to the main flow direction, thereby generating streamwise vortices. VGs can be arranged to create either co-rotating or counter-rotating vortices. This was invented by Taylor in the late forties. Widely used design criteria for VGs can be found in the book by Pearcey (1961). Inviscid theory based on the interaction between the different vortices and the surface was used to estimate the vortex paths. Lindgren (2002) recently used VGs to control separation in the plane asymmetric diffuser and a 10% increase in pressure recovery was achieved accompanied by significantly lowered pressure fluctuations. The drag induced by a VG increase with the VG size. This is a reason to try to minimize the VG size. Smaller VGs are utilizing the fact that the velocity profile is full in a ZPG turbulent boundary layer which means that high momentum is available very close to the surface. Several exploratory studies on smaller VGs, in terms of flow visualization and pressure recovery, have been performed. Rao & Kariya (1988) compared submerged devices to large scale VGs for separation control. None of the submerged types were larger than about 60% of the local boundary layer thickness. The submerged devices showed a better pressure recovery presumably due to less parasite drag. For a

review, see Lin (2000). Lin *et al.* (1989) (see also Lin *et al.* (1990)) investigated submerged VGs in a separated flow over a backward facing ramp. It was found that the submerged devices with relative height with respect to the boundary layer thickness h/δ=0.1 were effective but could not be placed more than 2δ upstream of the separation line due to a reduced downstream effectiveness. It was concluded that the sub-merged devices can not be smaller than y^+=150, which corresponded to h/δ=0.05. Lin (1999) positioned micro-VGs on the rear flap of a wing profile under landing-approach conditions. The conclusion was that the drag could be reduced with a micro-VG height of 0.18% of the air-foil chord length when placed at the downstream position of 25% of the flap chord length. The relative height of the VG compared to the boundary layer thickness, h/δ, is not clear. However, the term *micro*-VG is probably a bit misleading. Assuming δ to be on the order of 1% of the chord length, the VGs are h/δ=0.18. Shabaka *et al.* (1985), Mehta & Bradshaw (1988) and Pauley & Eaton (1988) have investigated the behaviour of streamwise vortices in more detail than the above studies, however, not in separated or APG flows but in ZPG boundary layers.

Model predictions for the flow field induced by triangular VGs were made by Smith (1994) to be used as a tool for VG design. The model predicted experimental data well and it was concluded that an increased benefit, in terms of increasing vortex strength, should be realized by an increased spanwise packing of VGs and by longer VGs. The most beneficial spanwise spacing was found to be D/d=2.4 (although values in the range D/d=2-6 was achieved). This is comparable to Pearcey (1961) D/d=4.

5.1.2. *Other passive techniques*

Lin *et al.* (1989), Selby *et al.* (1990) investigated the relative performance of short and long longitudinal grooves, transverse and swept grooves, VGs, sub-merged VGs and a passive porous surface by means of wall static-pressure measurements and flow visualization for reattachment control in a back-ward facing ramp. Longitudinal and transverse grooves were very successful with up to 66% reduction of the reattachment length. The transverse grooves substi-tute the large separated region for small regions which creates a wall slip layer which is effective for separation control. They are most efficient if placed where the pressure gradient is strongest. The swept grooves and the passive porous surface on the other hand enhanced the separation. Lin *et al.* (1990) tested several passive techniques in the same setup. Large Eddy Break-up Device (LEBU) with a small positive angle of attack was successful. Arches and the Helmholtz resonator had little effect whereas a spanwise cylinder removed the separation but gave a larger additional drag.

Meyer *et al.* (1999) used perforated flaps to mimic the effect of bird feathers *i.e.* they are self-actuated when separation occurs and they limit the upstream

growth of the separated region, increasing the lift by approximately 10-20%. These do not give any additional drag when separation is not present.

Nakamura & Ozono (1987) conducted an investigation where different amounts of free-stream turbulence (FST), generated by means of grids in a wind-tunnel experiment, shortened the separation bubble on a blunt flat plate. Kalter & Fernholz (2001) observed the same thing in a turbulent APG separation bubble.

5.2. Active techniques

Recent separation control techniques are based on active methods. The reason for choosing an active method is that it can be turned off when it is not needed as opposed to passive techniques which are usually based on fixed devices which induce a parasite drag at all times.

5.2.1. Blowing

Momentum injection parallel to the wall, so called tangential blowing, have been employed for a long time on fighter planes. Johnston (1990) instead investigated wall jets introducing streamwise vortices and showed that skewed pairs of jets could generate the same spanwise mean wall shear-stress as a fixed VG in a ZPG turbulent boundary layer. Measurements of mean velocity profiles at different spanwise positions show that streamwise vortices could be created. By using thermal tufts, measuring the backflow in separated flow, it was shown that the separation could be reduced. This means that active VGs can replace passive ditto and thereby eliminate the parasite drag at off-conditions, see also Lin *et al.* (1990).

5.2.2. Suction

Another technique is to apply suction which directs the flow towards the surface where the boundary layer separates. The low momentum fluid is essentially removed. This technique was applied in the present experimental setup, see figure 8.1, to prevent the boundary layer on a curved surface from separation.

5.2.3. Periodic forcing

Bar-Sever (1989) employed an oscillating wire on an airfoil which excited transverse velocity fluctuations, introducing large scale vortical structures which enhanced mixing and reentrainement of momentum in the separated region. The mean reverse flow was moved downstream and the u_{rms} level increased with a broader peak closer to the surface. Spectral measurements showed a large peak at the forcing frequency but not at the sub-harmonics. These results were true for a non-dimensional forcing frequency $0.4 \leq fC/U_\infty \leq 0.8$ indicating that structures larger than the chord length C are to large to be effective.

Combining the two techniques of blowing and suction, spanwise vorticity is introduced without a net massflow. Kiya *et al.* (1997) applied sinusoidal forcing at the corner of a blunt circular cylinder to affect the separated flow. The optimal frequency was found to scale with the natural frequency.

Elsberry *et al.* (2000) conducted measurements in a flow similar to Stratford (1959b,a), *i.e.* on the verge of separation. The flow was periodically forced through a spanwise slit which resulted in a lower value of the shape-factor, a reduced boundary layer thickness and an increase in the wall shear-stress.

Yoshioka *et al.* (2001b,a) used this technique for control of a separating flow over a backward facing step. The slit position was at the corner *i.e.* at the fixed separation line. The conclusion was that there is an optimal non-dimensional forcing frequency corresponding to a Strouhal number of $St \approx 0.2$, based on the centerline velocity and step height. The reattachment length was shortened by 30% in this case. It was suggested that for the optimal St the vortices impinge on the wall close to reattachment. A lower frequency gave vortices which impinged at the wall downstream of reattachment, which is in line with Bar-Sever (1989), and a too high frequency had the opposite effect. The presence of the vortices also changed the mean flow. There was a region of large strain between two vortices which altered the production rate and increased the momentum transfer of turbulence. Sonnenberger (2002) used sinusoidal forcing with an amplitude of 88% of the free-stream velocity upstream of a fence for separation control. The reattachment length was reduced by 35%. Microphones were used to measure the pressure difference upstream and downstream of the fence and it was shown that the pressure difference is correlated to the length of the separated region, information which is planned to be used in reactive control. Herbst & Henningson (2003) conducted a DNS with a similar case to Skote (2002) and controlled the separation bubble with blowing and suction through a slit. It was observed that a rather high amplitude is needed and that it is optimal to have the slit as close as possible to the mean separation point. F. Grewe (2003) (private communication) have done many preliminary tests on active control of a mild APG separation bubble. Blowing and suction utilized by loud speakers connected via tubing to a spanwise slit was employed. The forcing frequency was chosen to coincide with the natural frequency of the separated shear layer. The amplitude of the cross-flow was twice the free-stream velocity at the maximum. Phase averaged PIV measurements showed that spanwise vorticity was introduced which reduced the maximum backflow from 90% to 60%. The length of the mean reverse flow region was decreased by 50% compared to the unforced case. The slit was also divided into sections which could be forced successively out of phase, causing a three dimensional vorticity. This was shown to be more efficient than the two-dimensional case for an optimal spanwise spacing between the sections. The maximum backflow coefficient is reduced to 12% (*i.e.* the mean backflow is eliminated) for a spanwise spacing similar to that in the VG case in paper 4 and 5, *i.e.* as suggetsed by Pearcey

(1961). Reactive control is planned based on a new MEMS fence, see Schober *et al.* (2002), which is capable of measuring the instantaneous wall shear-stress inside the separation bubble.

CHAPTER 6

Separation prediction

It is desirable to be able to predict separation since this can have a large negative effect on the flow. This is a very difficult task, however, many different separation criteria have been suggested. For a two-dimensional steady boundary layer von Karman's momentum integral equation

$$\frac{\partial \theta}{\partial x} + (2 + H_{12})\frac{\theta}{U_\infty}\frac{\partial U_\infty}{\partial x} = c_f/2 \qquad (6.16)$$

expresses the balance between the loss of momentum, the pressure gradient and the wall shear-stress. This can be used to get an idea of the development of the boundary layer subjected to a pressure gradient, see for example Duncan *et al.* (1970) and Schlichting (1979). This approach can not handle separation as such, however the approximate position of separation can be determined based a critical value of H_{12} or where c_f becomes very small. The separation prediction by Stratford (1959b) was based on a non-dimensional pressure gradient, similar to the middle term in equation (6.16) (where a constant was allowed to depend on the sign of the 2nd derivative of the pressure gradient) together with a Reynolds number dependence. Another non-dimensional pressure gradient $\Gamma = \theta\frac{\partial c_p}{\partial x}Re_\theta^{0.25}$ has been suggested and according to Schlichting (1979) separation occurs at Γ=-0.06. Others have tried to relate separation to the boundary layer characteristics in terms of H_{12} and δ_*/δ, see Sandborn & Liu (1968) and Kline *et al.* (1983) (δ_*/δ=0.5 and H_{12}=4). Schofield (1986) claimed that separation can be related to their velocity scale u_s and that separation occurs at a value of u_s/u_∞=1.2±0.05, which gives a value of H_{12}=3.3. Mellor & Gibson (1966) suggests a value of H_{12}=2.35 and Dengel & Fernholz (1990) report a value H_{12}=2.85±0.1 from their experiment. The wide spread in the reported values reflect the fact that the separation point is difficult to determine accurately, however, separation may also depend on historical effects, 3D effects, Reynolds number etc. Sajben & Liao (1995) stated a criterion that describes the development of the boundary layer parameters in terms of a function $\sigma = \frac{\theta}{\delta - \delta_*}$. According to them, separation should occur when $\partial \sigma/\partial h$=0, h=1-1/$H_{12}$.

23

6.1. Computational Fluid Dynamics

Separation is also difficult to capture in simulations. The classical approach is that the turbulent velocity and pressure fields are decomposed into a mean and a fluctuating part with respect to time. This leads to that the Reynolds Averaged Navier-Stokes (RANS) equations contain additional unknowns, the Reynolds stress tensor, giving an unclosed set of equations which requires modeling. Turbulence modeling is a challenging task in complicated flow situations as turbulent boundary layer separation and such models need to be calibrated against accurate experimental data. This is one of the motivations for conducting the present measurements. An alternative to turbulence modeling and experiments is to solve the exact Navier-Stokes equations numerically in space and time, which is referred to as Direct Numerical Simulation (DNS). The limitation of this method is the large computational effort required which make simulations possible today only at fairly low Reynolds number. This is another reason for conducting turbulence measurements which can generally be conducted at higher Reynolds number. However, with the fast development of modern computers and increased computational speed, DNS has become an important tool in turbulence research. Another remedy for the shortcomings of DNS is to simulate only the large scale structures in so called Large Eddy Simulations (LES) and model the small scales with sub-grid models.

6.1.1. *Direct numerical simulations*

Na & Moin (1998) conducted a DNS by applying a normal velocity on the upper edge of a square computational box, which caused separation and reattchment on the opposite wall. Their data is in overall agreement with experimental data showing the ability of simulations, however, the backflow coefficient in the vicinity of the wall was 100% which has never been observed experimentally. Skote (2002) conducted a DNS on a similar case focusing on the proper velocity scaling, see chapter 2. The flow was forced to reattach in order to match the inlet conditions since periodic boundary conditions were used, which might have an upstream influence on the separation.

6.1.2. *RANS modeling*

In turbulence modeling the Reynolds stress tensor

$$R_{ij} = \overline{u_i' u_j'} \qquad (6.17)$$

is modeled to achieve a closed set of equations, which can be solved by numerical methods. The exact transport equation for the Reynolds stress tensor is

$$\frac{DR_{ij}}{Dt} = P_{ij} - \epsilon_{ij} + \Pi_{ij} - \frac{\partial}{\partial x_m}\left(J_{ijm} - \nu \frac{\partial R_{ij}}{\partial x_m}\right). \qquad (6.18)$$

The rate of change of the Reynolds stresses is balanced by the production, the dissipation rate, the inter-component redistribution and the diffusion, or
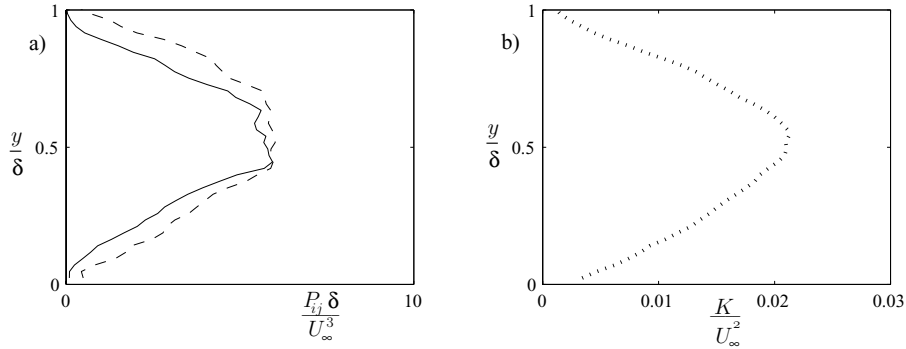
FIGURE 6.1. (a) The turbulence production terms $P_{uv}\delta/U_\infty^3$ (dashed line) and $P_{uu}\delta/U_\infty^3$ (line) and (b) the turbulence kinetic energy, $K=1/2\mathrm{Tr}(R_{ij})$ for the APG boundary layer in paper 4.

redistribution of energy in space. In two-dimensional boundary layer flow R_{ij} consist of four unknowns, the diagonal components, or the normal Reynolds stresses (which constitute the turbulence kinetic energy), and the Reynolds shear stress, $\overline{u'v'}$. To generate experimental results of turbulence quantities such as those in equation 6.18 is important for calibration of turbulence models and to increase the understanding of the turbulence structure itself. Bradshaw (1967) and Skåre & Krogstad (1994) presented Reynolds stress *budgets*, *i.e.* the different terms in equation (6.18), for APG equilibrium boundary layers and Simpson *et al.* (1981*b*) for a separated boundary layer. This is one benefit of conducting the present measurements. Figure 6.1 shows the turbulence kinetic energy and the turbulence production in the turbulent APG boundary layer measured with PIV presented in paper 4.

The simplest turbulence models are based on the eddy-viscosity concept of Boussinesq and the mixing-length hypothesis of Prandtl. These are algebraic expression relating the Reynolds stress tensor to the mean strain field. Two equation turbulence models are usually based on an equation for the turbulence kinetic energy together with an equation for a turbulent length scale, usually based on the rate of dissipation, so called k-ϵ models. Menter (1992) tested four different simple eddy-viscosity turbulence models and compared to experimental data from two APG flows, one mild and one separated case. The k-ω model overestimated the Reynolds shear-stress which lead to an underprediction of the separated region. The reason for the former was attributed to the eddy viscosity relation. Such models are today widely used by fluid dynamics engineers and they are implemented in many commercial codes. The instantaneous separation is a highly three-dimensional process without a clear separation and reattachment line and the two-dimensional mean bubble is merely
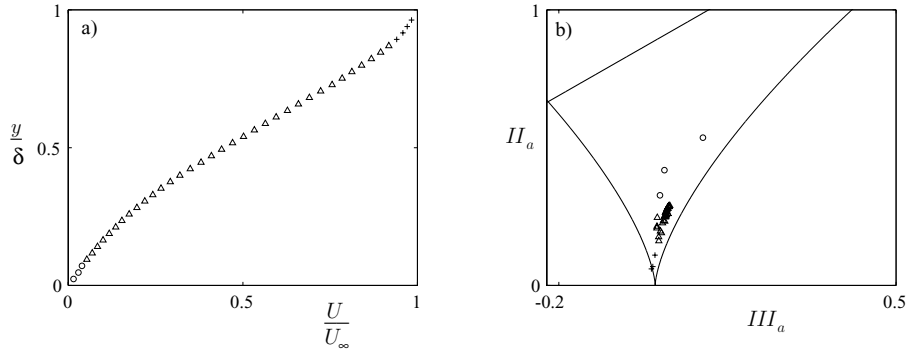
FIGURE 6.2. (a) The mean velocity profile and (b) the anisotropy invariant map for the APG boundary layer in paper 4. Note that the symbols indicate the wall distance.

a consequence of time averaging which means that turbulence modeling based on single-point closures will have difficulties to accurately predict separation. More advanced modeling is usually required if complex flow situations as the present one are to be well-predicted.

In Explicit Algebraic Reynolds Stress Models (EARSM) the differential equations for the evolution of the anisotropy

$$a_{ij} = \frac{R_{ij}}{K} - \frac{2}{3}\delta_{ij} \qquad (6.19)$$

are replaced by algebraic expressions. In Differential Reynolds Stress Models (DRSM) the exact equations are used. Henkes *et al.* (1997) tested four classes of turbulence models (k-ϵ, k-ω, EARSM and DRSM) and compared to the experimental data from Clauser (1954) and Skåre & Krogstad (1994) and to their own DNS data. It was reported that the DRSM gives the best agreement with experimental and DNS data.

The plane asymmetric diffuser is a flow case which is a challenging test-case for turbulence models with a large streamline curvature and fluctuating separation and reattachment. At the same time it is a well defined case using fully turbulent channel flow as inlet condition and a relatively simple geometry. An LES was conducted by Kaltenbach *et al.* (1999) which compared well with the mean velocity of Buice & Eaton (1996). Data using EARSM, compared fairly well with the PIV measurements from Lindgren (2002), however the extent of the separated region was under predicted.

A common way to the display the anisotropy state is by constructing the two invariants

$$II_a = a_{ij}a_{ji} \qquad III_a = a_{ij}a_{jk}a_{ki} \qquad (6.20)$$

26

and form the the so called Anisotropy Invariant Map (AIM) in the III_a, II_a-plane. All the realizable anisotropy states are bounded by $II_a^{1/2} = 6^{1/6} |III_a|^{1/3}$, corresponding to axisymmetric turbulence and $II_a = 8/9 + III_a$, corresponding to the two-component limit, shown as lines in figure 6.2. Figure 6.2 (b) shows the trajectory, when passing through an APG boundary layer in the wall-normal direction. The anisotropy state is close to the 2-component limit due to the fact that the wall-normal fluctuations are more affected by the wall than the streamwise and the spanwise components. The anisotropy state in the middle of the boundary layer is almost constant in a similar way to the logarithmic region in ZPG. In the outer wake-region the state changes towards the isotropic state in the free-stream (0,0). Turbulent APG boundary layers are overall less anisotropic than ZPG boundary layers according to Skote (2001).

CHAPTER 7

Experimental techniques

A wide span of scales pose large restrictions on both simulations and measurements of turbulent flows. As the Reynolds number increases, the span of scales increases and the smallest scales get smaller. Conducting measurements in turbulent flows is therefore not a simple task either. Typically, in a wind-tunnel experiment the smallest scales are of the order of mm-μm and ms-μs which makes it difficult to resolve the flow field spatially and temporarily. When the flow is separated, an additional measurement complication appears since the flow is reversed, requiring directionally sensitive measurement techniques.

7.1. Wall shear-stress measurements

In APG flows the wall shear-stress decreases and the viscous length scale is increased which makes it easier to spatially resolve the flow. However, wall-shear stress measurement techniques which can be used for such flows are limited. The indirect method of fitting a Clauser plot to the mean velocity profile in ZPG and mild APG is not possible to use in strong APG due to the vanishing logarithmic region. Preston tubes, which measure the total pressure close to the wall, also rely on the presence of a logarithmic region however, they can still be used as an indication of separation according to Muhammad-Klingmann & Gustavsson (1999). Wall pulsed-wires are mounted close enough to the wall to directly measure the velocity gradient. A hot-wire which is pulsed with a low frequency (limiting this technique to a sampling frequency of approximately 20 Hz) is surrounded by two sensor-wires in the upstream and downstream directions of the flow which makes it directionally sensitive, *i.e.* it can be used for backflow measurements. The accuracy is 4%. In the oil-film technique a drop of oil is placed at the wall. When the oil drop is illuminated with monochromatic light, the light is reflected in the wall and at the oil film surface and an interferration pattern is formed. The film is deformed by the wall shear-stress and the film thickness can be related to the interferration pattern, registered by a camera. The oil-film technique is directionally sensitive and gives the mean wall shear-stress with an accuracy of $\pm 4\%$. The surface fence consist of a small razor blade (typically on the order of 100μm) positioned in a cavity. The static pressure, measured upstream and downstream of the fence, is related to the wall shear-stress. This technique can be used in APG and separated flows. A

28

technique under development, which is capable of measuring the instantaneous wall shear-stress in backflow at a fairly high frequency, is the MEMS fence, see Schober *et al.* (2002). For a review on the ability of all these techniques for wall shear-stress measurements in APG flows, see Fernholz *et al.* (1996).

7.2. Velocity measurements

The experimental work of investigating the turbulence structure in APG started more than 50 years ago, Schubauer & Klebanoff (1950). However, using conventional hot-wires the instantaneous backflow could not be measured which restricted measurements to regions where this is zero. Measurements inside the separated region was first possible when Simpson *et al.* (1977) used a directionally sensitive Laser Doppler Anemometer (LDA) which made it possible to get a more clear view on the nature of turbulent separation, however, the errors were still fairly large. In LDA the measurement volume size is determiend by the lens system used and can be made rather small, typically of the order of 100μm. It can also give a high sampling rate and performs well also in high turbulence levels. Simpson *et al.* (1981b), Simpson *et al.* (1981a) and Shiloh *et al.* (1981) improved the accuracy of the LDA and also used pulsed hot-wires, see Bradbury & Castro (1971), for backflow measurements. Pulsed hot-wires also give a rather small measurement volume, however, the technique can have troubles in high turbulence levels. Another option is to use flying hot-wires, *i.e.* a hot-wire which is traversed in the direction of the flow with a known constant speed which removes the backflow with respect to the hot-wire. With the fast development of Particle Image Velocimetry (PIV), and in particular digital PIV, in the late nineties, this technique has become an new alternative for separated flows. The spatial resolution is not yet comparable to LDV and hot-wire and the temporal resolution is very poor, although time resolved PIV is under development. However, the ability of PIV for accurate turbulence measurements was shown by a direct comparison with the hot-wire technique in a ZPG boundary layer, see paper 1 and figure 7.1 (a). PIV also gives us information about the instantaneous flow field as opposed to conventional single-point measurement techniques. Below, an example of the use of PIV for detecting coherent structures is shown.

7.3. Measurements of turbulent structures using PIV

The signature of a hairpin vortex is revealed in figure 7.1 (b), when the mean velocity is subtracted showing only the superimposed turbulent fluctuations. A well-established fact is that low-speed streaks exist in the near-wall region ($y^+ \leq$20) of ZPG turbulent boundary layers. Such streaks are known to have a characteristic spanwise spacing of λ^+=100. It has been suggested that merging of such sub-layer streaks takes place outside the viscous sub-layer. Smith & Metzler (1981) observed how two adjacent streaks merged to one with twice the spanwise wave length at y^+=30 and Nakagawa & Nezu (1981) showed results
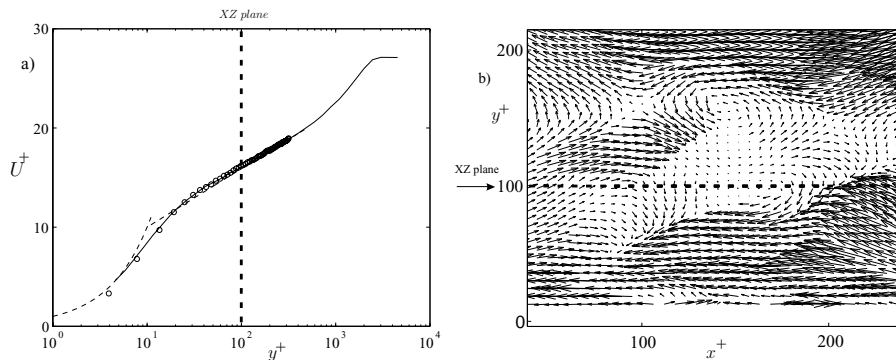
FIGURE 7.1. (a) The wall-normal mean velocity profile in inner variables. The line corresponds to hot-wire data obtained earlier in the same setup by Österlund (1999) and the symbols correspond to the PIV data presented in paper 1. The dashed line shows the wall-normal position of the PIV xz-plane measurements. (b) PIV velocity field showing the instantaneous foot print of a hairpin vortex. This was captured in connection with the data presented in paper 1.

further out from the wall which indicated that $\lambda^+=2y^+$ at $100\leq y^+\leq500$. To detect such streaks may require special sampling techniques. The two-point correlation function

$$R_{uu} = \frac{\overline{u(z)u(z+\Delta z)}}{\overline{u(z)^2(z+\Delta z)^2}} \tag{7.21}$$

is a way to investigate the spanwise structure of streaks. PIV measurements were done in the present work with the laser sheet aligned with the plate in the beginning of the logarithmic part of the boundary layer at $y^+=100$, see figure 7.1 (a), cutting through rising hairpin vortices, see figure 7.1 (b). Figure 7.2 (a) shows an example of an instantaneous low velocity streak. The auto-correlation of such streaks was evaluated in the following manner: R_{uu} was computed from each instantaneous velocity field where u' was predominantly negative (about 50% of the images). Thereafter, correlation functions showing a negative minimum, indicating the presence of a low speed streak, were selected and averaged. This technique is in essence equivalent to conditional sampling. R_{uu} indicates that there is an alternating positive and negative correlation at a spanwise peak-to-peak $\lambda^+=620$, see figure 7.2 (b). The data were also reprocessed with half the interrogation area size which did not have any effect on the measured streak spacing.
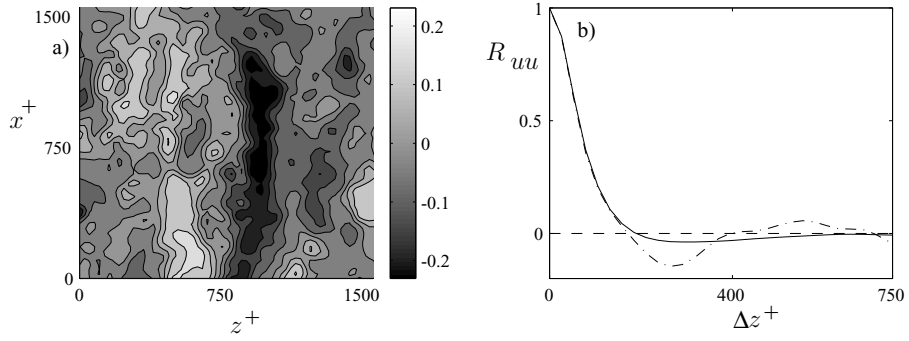
FIGURE 7.2. (a) Instantaneous low velocity streak around y^+=85-115 captured with PIV in a ZPG turbulent boundary layer. The contours are showing the turbulence intensity *i.e.* the instantaneous velocity fluctuation normalized by the free-stream velocity. (b) Spanwise correlation coefficient R_{uu}. The line corresponds to the averaged correlation from 607 PIV measurements and the dash-dotted line to the instantaneous correlation from the single PIV realization shown in (a).

CHAPTER 8

Present work

The object of the present study is a mild APG boundary layer with both separation and reattachment. There are many reasons for choosing this particular case. First, it is a flow case with large practical relevance since it is optimal in terms of maximum lift. From an experimental point of view, a mild separation with reattachment gives a fair chance of achieving a two-dimensional and well-defined flow. This has been found to be a difficultly in previous separation experiments and this may be one of the reasons for the wide spread in the existing experimental data on separating turbulent boundary layers. The aspect ratio between the spanwise width of the wind-tunnel and the boudary layer thickness (or bubble height) is also higher. Other factors of importance, if the data are to be used for validation of turbulence models, are to have a well-defined, repeatable and steady flow case with specified inlet- and free-stream conditions.

The present work includes:

- Design and manufacturing of a special APG wind-tunnel test section.
- Development of PIV measurement and evaluation techniques for boundary layer flow.
- Scaling of boundary layers with APG and separation.
- Studies on the turbulence structure of the separating boundary layer with control.

8.1. Experimental design

The experiments were carried out at KTH in a new closed loop wind-tunnel, see Lindgren & Johansson (2003). The test-section is interchangable and for the present experiments a special test-section was designed. A view from inside the test section is shown in figure 8.1. A flat plate consisting of four 1 m long 20 mm thick segments was mounted vertically (the picture is rotated $90°$) in the test section, 300 mm from one of the test section walls. At $x=1.25$m the test-section is diverged by means of a flexible wall (allowing a free choice of the wall shape) in order to achieve a decelerating flow. In order to force separation on the flat plate, suction was applied through holes in the curved wall. The suction is applied where the pressure gradient is strongest. The required suction rate

FIGURE 8.1. Test section seen from the inside in the present turbulent APG boundary layer setup. The flow is out of the picture. The curved flexible wall, seen in the top of the picture, where suction is applied, induces an APG on the flat plate (at the bottom of the picture).

was estimated based on the mass-flow rate in the wind-tunnel. The flat plate, the curved wall and the side walls were made in Plexiglas$^{\circledR}$ and Macrolon$^{\circledR}$ respectively to be able to use optical techniques such as LDV and PIV. The shape of the flexible curved wall and the suction flow rate were determined by aid of Cfx calculations of the boundary layer development. The design was guided by a pilot study, carried out in a smaller facility by Gustavsson (1999), Muhammad-Klingmann & Gustavsson (1999). The final shape of the flexible curved surface, which can be adjusted for different pressure gradients, was tuned using wall static pressure measurements, flow visualization by tufts and backflow measurements using LDV, to achieve a mild APG separation with reattachment. The flow is made to reattach on the flat plate by contracting the flexible wall towards the end of the test section. This results in a well-defined and steady separation bubble as seen in figure 3.3.

8.1.1. *Details of the experimental setup*

The suction was applied through 1300 holes with a diameter of 5 mm, distributed over an area of 0.75 m^2, *i.e.* 3.4% of the total suction area is covered by holes. This was shown to be enough to get a homogeneous free-stream velocity. Approximately 6-7% of the total flow rate (based on the flow rate above the flat plate) was estimated to be removed based on LDV measurements at the fan outlet. This is returned into the wind-tunnel downstream of the test-section through a pressure equalizer slit.

The first segment of the flat plate has a 0.2 m long symmetric super-elliptic leading edge. To be able to control and assure a non-separated leading edge flow, the last 0.5 m of the last plate segment was used as a flap. In order

to obtain a well defined and spanwise homogeneous position of the laminar to turbulent transition a 0.4 mm high zig-zag tape was used. It was placed 0.25 m downstream of the tip of the leading edge (at Re_x=4.4·10^5 based on the free-stream velocity). This arrangement assured a fully developed turbulent ZPG boundary layer as a well defined inlet condition well upstream of the expanding part of the test-section. The flat plate is equipped with 48 pressure taps evenly distributed in the downstream direction at every 0.1 m downstream of the first meter. Pressure taps are also placed in the spanwise direction 0.175 m off the centerline at every second tap position after the first meter. The spanwise homogeneity of the free-stream velocity was first estimated by such wall static pressure measurements. Measurements of the V component in the free-stream were made with PIV at the position of the bubble. Further, the spanwise homogeneity was estimated using PIV measurements in the spanwise direction (xz-planes). In the free-stream, above the separated region, the streamwise mean velocity was shown to be two-dimensional within ±0.15% from the centerline to a position 150 mm off the centerline. Close to the wall (y/δ=0.09) at separation, where the flow is much more sensitive, U/U_∞=0.04±0.02, see paper 5. The Reynolds shear-stress in this plane, which should be zero in a 2D flow, shows scattered values around zero which are at the maximum one order of magnitude smaller than the primary Reynolds shear stress at the same position.

8.2. The use of PIV for accurate boundary layer measurements

The major contribution to the field of PIV research is the accuracy investigation of turbulence measurements through direct comparisons with highly accurate hot-wire data in a ZPG case presented in paper 1. It is shown that by careful design of the experiment and correctly applied validation criteria, PIV is a serious alternative to conventional techniques such as hot-wire and LDV for well-resolved accurate turbulence measurements at high Reynolds numbers. The results from the simulations presented in paper 2 constitute useful guidelines for error estimations and symptoms of peak-locking and when these errors are to be expected.

Different seeding techniques were tested for PIV measurements in turbulent boundary layers. In the pilot study, Muhammad-Klingmann & Gustavsson (1999), a slit in the flat plate was used to introduce smoke into the boundary layer. It was observed that the free-stream was not effectively seeded by this technique. Holm & Gustavsson (1999) used the same technique and observed disturbances in the boundary layer originating from a pressure difference over the smoke injection slit. In the ZPG experiment, presented in paper 1, smoke was injected by means of a traversable pipe placed in the stagnation chamber at a height which assures that the smoke hits the leading edge. The smoke is thereby localized to a thin layer near the plate and is entrained into the

boundary layer. With this technique, the amount of smoke and hence the contamination of the wind-tunnel is minimized without introducing disturbances into the boundary layer. The easiest and most successful seeding technique is to fill the wind-tunnel by injecting a large amount of smoke in the stagnation chamber or after the test section and letting it recirculate in the tunnel. The boundary layer then becomes homogeneously seeded due to the turbulent mixing. This technique was used for all the separation and control measurements.

8.3. Scaling in separating APG turbulent boundary layer flow

Self-similarity scaling in a separating APG turbulent boundary layer is an important tool for an increased understanding of this complex flow. At the same time, it constitutes valuable information for developers of turbulence models. The proper velocity scaling for the outer region in a strong separated APG boundary layer is still debated. Discussion has also been restricted mostly to the mean velocity profile and less attention has been paid to experimental guidance for the proper scaling of the Reynolds shear-stress, of particular interest for turbulence modeling purposes. The scaling by Coles (1956) is in fair agreement with the present data far upstream of separation whereas closer to separation it is not predicting the data well. This is in line with earlier data, see for example Dengel & Fernholz (1990). It is showed in the present experiments that scaling based on a velocity scale related to the local pressure gradient gives similarity not only for the mean velocity but also to some extent for the Reynolds shear-stress. This velocity scale appears naturally in the scaled turbulent boundary layer equation and was originally suggested by Mellor & Gibson (1966) for equilibrium flow at the position of separation. The same degree of similarity was found both for the mean velocity profile and the Reynolds shear-stress using the Perry-Schofield velocity scale. Therefore, it must be correlated to the above scaling which explains the earlier success of the Perry-Schofield velocity scale and the claimed relation between this velocity scale and the maximum Reynolds shear-stress. The present streamwise mean velocity profiles do not fall exactly on the asymptotic profile suggested by earlier authors which shows that profile similarity achieved within an experiment is not universal. This complex flow is obviously governed by parameters which are still not accounted for in the proposed velocity scales, one such might be historical effects.

8.4. Control and turbulence structure of a separating APG boundary layer

Control of a separation is important for increasing the efficiency in many technical applications. A deeper understanding of the interaction between streamwise vortices and a separating APG boundary layer has been achieved in terms of turbulence structure and instantaneous vortex behaviour. PIV measurements

made it possible to capture the vortices instantaneously in the plane of rotation. It was shown that the mean size of the vortices increases, the maximum vorticity decreases as the circulation is conserved in the downstream direction. The vortices are non-stationary with movements in both directions. The spanwise movements are larger than those in the wall-normal direction, presumably due to the presence of the wall. These movements contribute to high levels of the Reynolds stresses in this plane, centered around the mean vortex positions. These movements also imply that the mean vortex is smeared out, *i.e.* the instantaneous vortices are generally smaller and stronger and are also subjected to vortex stretching. The high levels of fluctuations around the mean vortex centers decrease in the downstream direction at the same time as the spanwise component increases in the downstream direction in the near-wall region. The latter fact might be connected to the induced secondary vorticity below the vortices due to the no-slip condition of W. Initially non-equidistant vortices become and remain equidistant and are confined to the boundary layer. The vortices rearrange the boundary layer flow and the streamwise mean velocity profiles become S-shaped in the wall-normal direction with a spanwise modulation. At spanwise positions of symmetry, the turbulence production has large peaks in the near-wall and outer regions whereas the middle region is a region of low shear leading to a lower turbulence kinetic energy and a relaxed nearly isotropic turbulence state. The spanwise gradient of the streamwise mean velocity cause production and high levels of turbulence at spanwise positions between the symmetry planes. The amount of initial streamwise circulation was found to be a crucial parameter for successful separation control whereas the exact streamwise position of the vortex generators, and their relative height with respect to the local boundary layer thickness, is of secondary importance. Even with relatively small VGs positioned further downstream, the overall wall shear-stress is increased to a value which is larger than in a ZPG boundary layer. It is speculated that it is important to create an environment where the self-susstained turbulence re-generation mechanism can withstand the pressure gradient. The vortices which are induced when the pressure gradient has already seriously affected the shape of the mean velocity profile at the vortex generator position are not as efficient. The vortices were found to grow with the boundary layer in the downstream direction, and the downstream vortex size is determined by the vortex generator height. The strong three-dimensionality induced by the vortices is reduced in the downstream direction and the asymptotic state is a two-dimensional boundary layer with S-shaped mean velocity profiles in the wall-normal direction.

8.5. Outlook and suggestions for future work

The generality of the pressure gradient based velocity scaling should be tested. The influence of upstream conditions such as the Reynolds number, the shape of pressure gradient, the boundary layer development and extent of the separated

region, should be investigated. This would maybe lead to a better understanding of what paramaters govern this flow. Lie group symmetry methods for ZPG boundary layers, see Lindgren (2002), should be extended to APG and separation for comparison with the present data base. Smaller vortex generators should be tested to further investigate the importance of the vortex size on the separation elimination ability. More advanced active or reactive control, should be implemented based on the achieved knowledge of the effect of streamwise vortices.

Acknowledgments

References

ADRIAN, R. J., MEINHART, C. D. & TOMKINS, C. D. 2000 Vortex organization in the outer region of the turbulent boundary layer. *J. Fluid Mech.* **422**, 1–54.

ALVING, A. & FERNHOLZ, H. 1995 Mean velocity scaling in and around a mild turbulent separation bubble. *Phys. Fluids* **7** (8), 1956–1969.

ALVING, A. & FERNHOLZ, H. 1996 Turbulence measurements around a mild separation bubble and downstream of reattachment. *J. Fluid Mech.* **322**, 297–328.

BAR-SEVER, A. 1989 Separation control on an airfoil by periodic forcing. *AIAA J.* **27** (6), 820–821.

BRADBURY, L. J. S. & CASTRO, I. P. 1971 A pulsed-wire technique for velocity measurements in highly turbulent flow. *J. Fluid Mech.* **22**, 679–687.

BRADSHAW, P. 1967 The turbulent structure of equilibrium turbulent boundary layers. *J. Fluid Mech.* **29**, 625–645.

BUICE, C. U. & EATON, J. K. 1996 Experimental investigation of flow through an asymmetric plane diffuser. *CTR, Ann. Research Briefs* pp. 243–248.

CASTILLO, L. & GEROGE, W. 2001 Similarity analysis for turbulent boundary layer with pressure gradient: The outer flow. *AIAA J.* **39** (1), 41–47.

CLAUSER, F. 1954 Turbulent boundary layers in adverse pressure gradients. *J. of Aero. Sci.* **21**, 91–108.

COLES, D. 1956 The law of the wake in the turbulent boundary layer. *J. Fluid Mech.* **1**, 191–226.

DENGEL, P. & FERNHOLZ, H. 1990 An experimental investigation of an incompressible turbulent boundary layer in the vicinity of separation. *J. Fluid Mech.* **212**, 615–636.

DIANAT, M. & CASTRO, I. 1989 Measurements in separated boundary layers. *AIAA J.* **27** (6), 719–723.

DIANAT, M. & CASTRO, I. 1991 Turbulence in a separated boundary layer. *J. Fluid Mech.* **226**, 91–123.

DUNCAN, W., THOM, A. & YOUNG, A. 1970 *Mechanics of Fluids*. Edward Arnold Printers Ltd. London.

ELSBERRY, K., LOEFFLER, J., ZHOU, M. D. & WYGNANSKI, I. 2000 An experimental study of a boundary layer that is maintained on the verge of separation. *J. Fluid Mech.* **423**, 227–261.

Fernholz, H. H., Janke, G., Schober, M., Wagner, P. M. & Warnack, D. 1996 New developments and applications of skin-friction measuring techniques. *Meas. Sci. Technol.* **7**, 1396–1409.

Fukugata, K. & Kasagi, N. 2002 Active feed-back control of turbulent pipe flow. In *3rd Symposium on Smart Control of Turbulence*.

Gad-El-Hak, M. 2000 *Flow Control Passive, Active, and reactive Flow Management*. Cambridge University press.

Gad-El-Hak, M. & Bushnell, D. 1991 Status and outlook of separation control. *AIAA Paper 91-0037* .

Gustavsson, J. 1999 Turbulent flow separation. Master's thesis, Dept. Mechanics, Royal Institute of Technology, Stockholm.

Hancock, P. E. 2000 Low reynolds number two-dimensional separated and reattaching turbulent shear flow. *J. Fluid Mech.* **410**, 101–122.

Henkes, R. A. W. M., Skote, M. & Henningson, D. S. 1997 Application of turbulence models to equilibrium boundary-layers under adverse pressure gradient. In *11th Symposium on Turbulent Shear Flows, Grenoble France, 33:13-33:18*.

Herbst, A. H. & Henningson, D. 2003 Influence of periodic exitation on a turbulent separation bubble. *Tech. Rep.*. PSCI no. 30.07.

Högberg, M. 2001 Optimal control of boundary layer transition. PhD thesis, Dept. Mechanics, Royal Institute of Technology, Stockholm.

Holm, R. & Gustavsson, J. 1999 A PIV study of separated flow around a 2D airfoil at high angles of attack in a low speed wind tunnel. *Tech. Rep.*. FFA TN 1999-52.

Hoyt, J. W. & Sellin, R. H. J. 1991 Polymer threads and drag reduction. *Rheologica Acta* **30**, 307–315.

Hudy, L. M. & Naguib, A. M. 2003 Wall-pressure-array measurements beneath a separating/reattaching flow region. *Phys. Fluids* **16** (12), 2068–2074.

Johnston, J. P. 1990 Vortex generator jets - means for separation control. *AIAA J.* **28** (6), 989–994.

Kader, B. A. & Yaglom, A. M. 1978 Similarity treatment of moving-equilibrium turbulent boundary layers in adverse pressure gradients. *J. Fluid Mech.* **89**, 305–342.

Kaltenbach, H. J., Fatica, M., Mittal, R., Lund, T. & Moin, P. 1999 Study of flow in a planar asymmetric diffuser using large-eddy simulation. *J. Fluid Mech.* **390**, 151–185.

Kalter, M. & Fernholz, H. H. 2001 The reduction and elimination of a closed separation region by free-stream turbulence. *J. Fluid Mech.* **446**, 271–308.

Kiya, M. & Sasaki, K. 1983 Structure of a turbulent separation bubble. *J. Fluid Mech.* **137**, 83–113.

Kiya, M., Shimizu, M. & Mochizuki, O. 1997 Sinusoidal forcing of a turbulent separation bubble. *J. Fluid Mech.* **342**, 119–139.

Kline, S., Bardina, J. & Strawn, R. 1983 Correlation of the detachment of two-dimensional turbulent boundary layers. *AIAA J.* **21** (1), 68–73.

Lin, J. 1999 Application of micro-vortex generators for turbulent flow separation control. In *IUTAM Symposium on Mechanics of Passive and Active Technique Flow Control, 81-88*.

Lin, J., Howard, F. & Selby, G. 1989 Turbulent flow separation control through passive techniques. *AIAA Paper 89-0976* .

Lin, J. C. 2000 Review of research on low-profile vortex generators to control boundary-layer separation. *Prog. In Aerospace Sci.* **38**, 389–420.

Lin, J. C., Howard, F. G., Bushnell, D. M. & Selby, G. V. 1990 Investigation of several passive and active methods for turbulent separation control. *AIAA Paper 90-1598* .

Lindgren, B. 2002 Flow facility design and experimental studies of wall-bounded turbulent shear-flows. PhD thesis, Dept. Mechanics, Royal Institute of Technology, Stockholm.

Lindgren, B. & Johansson, A. V. 2003 Evaluation of a new wind-tunnel with expanding corners. *Accepted for publication in Exp. in Fluids* .

Lundell, F. 2003 Experimental studies of bypass transition and its control. PhD thesis, Dept. Mechanics, Royal Institute of Technology, Stockholm.

McDonald, H. 1969 The effect of pressure gradient on the law of the wall in turbulent flow. *J. Fluid Mech.* **35**, 311–336.

Mehta, R. D. & Bradshaw, P. 1988 Longitudinal vortices imbedded in turbulent boundary layers. Part 2. Vortex pair with "common flow" upwards. *J. Fluid Mech.* **188**, 529–546.

Mellor, G. L. 1966 The effects of pressure gradients on turbulent flow near a smooth wall. *J. Fluid Mech.* **24**, 255–274.

Mellor, G. L. & Gibson, D. M. 1966 Equilibrium turbulent boundary layers. *J. Fluid Mech.* **24**, 225–253.

Menter, F. R. 1992 Performance of popular turbulence models for attached and separated pressure gradient flows. *AIAA J.* **30** (8), 2066–2072.

Meyer, R., Bechert, D. W. & Hage, W. 1999 Windtunnel experiments with artificial bird feathers for passive separation control on airfoils. In *IUTAM Symposium on Mechanics of Passive and Active Technique Flow Control*.

Muhammad-Klingmann, B. & Gustavsson, J. 1999 Experiments on turbulent flow separation. *IMechE C557/153/99* .

Na, Y. & Moin, P. 1998 Direct numerical simulation of a separated turbulent boundary layer. *J. Fluid Mech.* **374**, 379–405.

Nakagawa, H. & Nezu, I. 1981 Structure of space-time correlations of bursting phenomena in an open-channel flow. *J. Fluid Mech.* **104**, 1–43.

Nakamura, Y. & Ozono, S. 1987 The effects of turbulence on a separated and reattaching flow. *J. Fluid Mech.* **178**, 477–490.

Österlund, J. 1999 Experimental studies of zero pressure-gradient turbulent boundary-layer flow. PhD thesis, Dept. Mechanics, Royal Institute of Technology, Stockholm.

Österlund, J., Lindgren, B. & Johansson, A. V. 2002 Flow structures in zero pressure-gradient turbulent boundary layers at high reynolds number. *Submitted to European Journal of Mechanics B/Fluids* .

Pauley & Eaton 1988 Experimental study of the development of longitudinal vortex pairs embedded in a turbulent boundary layer. *AIAA J.* **26** (7), 816–823.

Pearcey, H. H. 1961 *Shock-induced separation and its prevention by design and*

boundary-layer control. In Boundary Layer and Flow Control, its Principle and Applications, Vol 2, Edited by G. V. Lachmann. Pergamon press, Oxford, England.

Perry, A. 1966 Turbulent boundary layers in decreasing adverse pressure gradients. *J. Fluid Mech.* **26**, 481–506.

Perry, A., Bell, J. B. & Joubert, P. N. 1966 Velocity and temperature profiles in adverse pressure gradient turbulent boundary layers. *J. Fluid Mech.* **26**, 299–320.

Perry, A. & Schofield, W. 1973 Mean velocity and shear stress distribution in turbulent boundary layers. *Phys. Fluids* **16** (12), 2068–2074.

Rao, D. & Kariya, T. 1988 Boundary-layer submerged vortex generators for separation control - an exploratory study. *AIAA Paper 88-3546* .

Ruderich, R. & Fernholz, H.-H. 1986 An experimental investigation of a turbulent shear flow with separation, reverse flow and reattachment. *J. Fluid Mech.* **163**, 283–322.

Sajben, M. & Liao, Y. 1995 Criterion for the detachment of laminar and turbulent boundary layers. *AIAA J.* **33** (11), 2114–2119.

Sandborn, V. & Liu, C. 1968 On turbulent boundary-layer separation. *J. Fluid Mech.* **32** (2), 293–304.

Schlichting, H. 1979 *Boundary Layer Theory*. McGraw-Hill.

Schober, M., Obermeier, E., Papen, T., Pirskawetz, S. & Fernholz, H.-H. 2002 A MEMS fence for time resolved skin-friction measurements in separated flows. In *Advances in turbulence IX* .

Schofield, W. 1981 Equilibrium boundary layers in moderate to strong adverse pressure gradient. *J. Fluid Mech.* **113**, 91–122.

Schofield, W. 1986 Two-dimensional separating turbulent boundary layers. *AIAA J.* **24** (10), 1611–1619.

Schubauer, G. & Spangenberg, W. 1960 Forced mixing in boundary layers. *J. Fluid Mech.* **8**, 10–32.

Schubauer, G. B. & Klebanoff, P. S. 1950 Investigation of separation of the turbulent boundary layer. *National Advisory Committee for Aeronautics* **Report 1030**, 689–708.

Selby, G., Lin, J. & Howard, F. 1990 Turbulent flow separation control over a backward-facing ramp via transverse and swept grooves. *J. of Fluids Eng., Tech. Briefs* .

Shabaka, I. M. M. A., Mehta, R. D. & Bradshaw, P. 1985 Longitudinal vortices imbedded in turbulent boundary layers. Part 1. Single vortex. *J. Fluid Mech.* **155**, 37–57.

Shiloh, K., Shivaprasad, B. & Simpson, R. 1981 The structure of a separating turbulent boundary layer. Part 3. transverse velocity measurements. *J. Fluid Mech.* **113**, 75–90.

Simpson, R. 1989 Turbulent boundary-layer separation. *Ann. Rev. Fluid Mech.* **21**, 205–234.

Simpson, R., Chew, Y. & Shivaprasad, B. 1981a The structure of a separating turbulent boundary layer. Part 2. Higher-order turbulent statistics. *J. Fluid Mech.* **113**, 53–73.

SIMPSON, R., CHEW, Y. & SHIVAPRASAD, B. 1981b The structure of a separating turbulent boundary layer.Part 1. Mean flow and Reynolds stress. *J. Fluid Mech.* **113**, 23–51.

SIMPSON, R., STRICKLAND, J. H. & BARR, P. W. 1977 Features of a separating turbulent boundary layer in the vicinity of separation. *J. Fluid Mech.* **79**, 553–594.

SKÅRE, P. & KROGSTAD, P. 1994 A turbulent equilibrium boundary layer near separation. *J. Fluid Mech.* **272**, 319–348.

SKOTE, M. 2001 Studies of turbulent boundary layer flow through direct numerical simulation. PhD thesis, Dept. Mechanics, Royal Institute of Technology, Stockholm.

SKOTE, M. 2002 Direct numerical simulation of a separated turbulent boundary layer. *J. Fluid Mech.* **471**, 107–136.

SMITH, C. R. & METZLER, S. P. 1981 The characteristics of low-speed streaks in the near wall region of a turbulent boundary layer. *J. Fluid Mech.* **129**, 27–54.

SMITH, F. T. 1994 Theoretical prediction and design for vortex generators in turbulent boundary layers. *J. Fluid Mech.* **270**, 91–131.

SMITH, R. E. & TIEDERMAN, W. G. 1991 The mechanism of polymer thread drag reduction. *Rheologica Acta* **30**, 103–113.

SONNENBERGER, R. 2002 Simultaneous PIV and pressure measurements upstream and downstream of a fence. In 11th *International Symposium Applications of laser techniques to fluid mechanics*.

STRATFORD, B. 1959a An experimental flow with zero skin friction throughout its region of pressure rise. *J. Fluid Mech.* **5**, 17–35.

STRATFORD, B. 1959b The prediction of separation of the turbulent boundary layer. *J. Fluid Mech.* **5**, 1–16.

TÖRNBLOM, O. 2003. Experimental study of the turbulent flow in a plane asymmetric diffuser. Licentiate thesis, Dept. Mechanics, Royal Institute of Technology, Stockholm.

TOWNSEND, A. A. 1961 Equilibrium layers and wall turbulence. *J. Fluid Mech.* **11**, 97–120.

WATMUFF, J. H. & WESTPHAL, R. W. 1989 A turbulent boundary layer at low Reynolds number with adverse pressure gradient. In 10th *Australianasian Fluid Mechanics Conference-University of Melbourne*.

YAGLOM, A. M. 1979 Similarity laws for constant-pressure and pressure-gradient turbulent wall flows. *Ann. Rev. Fluid Mech.* **11**, 505–540.

YOSHINO, T., TSUDA, M., SUZUKI, Y. & KASAGI, N. 2002 Toward development of feed-back control system for wall turbulence with mems sensors and actuators. In 3rd *Symposium on Smart Control of Turbulence*.

YOSHIOKA, S., OBI, S. & MASUDA, S. 2001a Organized motion in periodically perturbed separated flow over backward-facing step. *International Journal of Heat and Fluid Flow* **22**, 301–307.

YOSHIOKA, S., OBI, S. & MASUDA, S. 2001b Turbulence statistics of periodically perturbed separated flow over backward-facing step. *International Journal of Heat and Fluid Flow* **22**, 393–401.

Zhou, J., Adrian, J., Balachandar, S. & Kendall, T. M. 1999 Mechanisms for generating coherent packets of hairpin vortices in channel flow. *J. Fluid Mech.* **387**, 353–396.